PNAS
www.pnas.org

Supplementary Information for

Horsefly object-directed polarotaxis is mediated by a stochastically distributed ommatidial subtype in the ventral retina

Andrej Meglič, Marko Ilić, Primož Pirih, Aleš Škorjanc, Martin F. Wehling, Marko Kreft, Gregor Belušič

Corresponding author: Gregor Belušič
Email: gregor.belusic@bf.uni-lj.si

This PDF file includes:

Figs. S1 to S3
Supplementary Materials and Methods
References for SI

Other supplementary materials for this manuscript include the following:

Movies S1 to S3
Datasets S1

Available at Figshare: https://dx.doi.org/10.6084/m9.figshare.8222444

www.pnas.org/cgi/doi/10.1073/pnas.1910807116

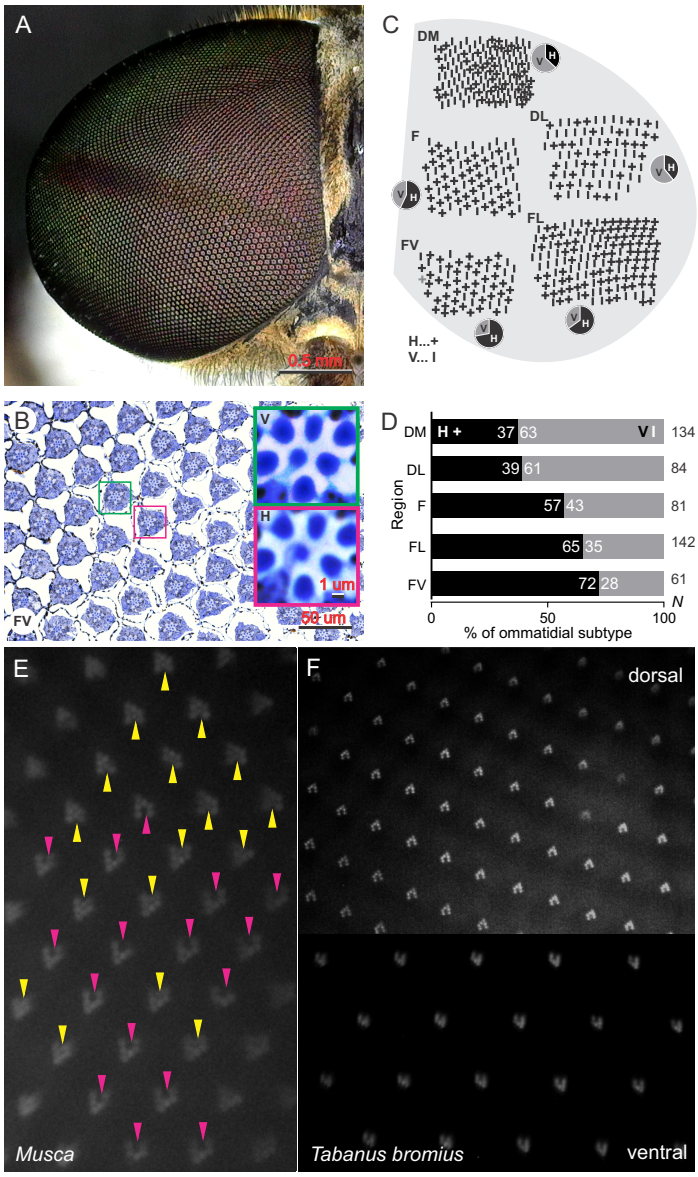

Fig. S1. Regionalization of the retina of a horsefly female.

(*A*) Macro photograph of the right compound eye of a *Tabanus bromius* female. The dark band at the middle coincides with the eye equator. The equator is tilted from the horizon by ~20°, meaning that the „vertical" and „horizontal" rhabdomeres are positioned at absolute angles 20° and 110°. (*B*) Light micrograph of a distal section of the frontal retina. Insets, magnified rhabdoms containing R7 with vertical (V) or horizontal (H) microvilli, allowing to classify all ommatidia in the section as V- or H-type. (*C*) Distribution of the two ommatidial types H (indicated with +, representing orthogonal analyzer R7,8 pair for polarization vision) and V (indicated with I, representing parallel R7,8 pair for color vision) in different parts of the retina: DM, dorsomedian, DL, dorsolateral, F, frontal, FV, frontoventral, FL, frontolateral. The two types are distributed semistochastically, with a pronounced dorsoventral gradient. Fractions for each part are indicated with pie charts. The size of each analyzed region is ~200 x 300 µm; not drawn to scale. (*D*) Fractions of H and V ommatidia in the different parts of the retina; numbers in bars indicate percents; numbers of ommatidia, counted in each part are indicated at the right. (*E*) Visualisation of *pale* (pink arrows, pointing to the nonfluorescing central rhabdomeres) and *yellow* (yellow arrows, pointing to the fluorescing central rhabdomeres) ommatidia in the compound eye of a muscid fly, using corneal neutralization with water immersion, UV epi-illumination and blue-green fluorescence. (*F*) Compound eye of a *T. bromius* female, observed with the same technique as in (*D).* The central rhabdomeres do not emit any fluorescence and could not be identified as *yellow* and *pale*.

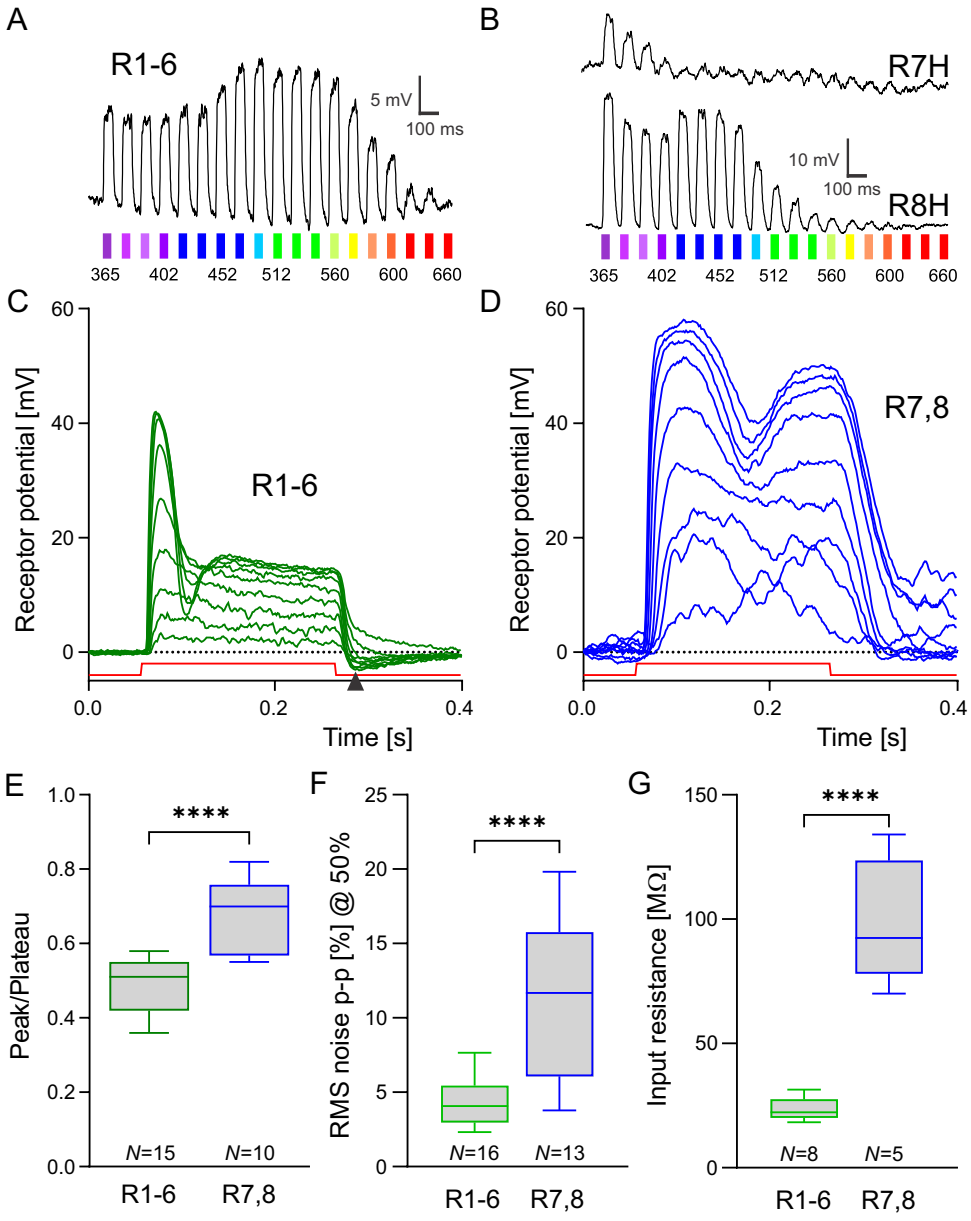

Fig. S2. Electrophysiological identification of impaled cells.

(*A, B*) Identification of the impaled cells with a fast spectral scan, using a sequence of LED lamps. Representative responses of single cells; LED wavelengths are indicated below the colored stimuli (the average wavelength step between consecutive LEDs is 15 nm). (*A*) Peripheral receptor R1-6, peaking in the green. (*B*) Central receptor R7 (top) and R8 (bottom trace), peaking in the UV and blue, respectively. (*C*) Representative receptor potential of R1-6, stimulated with a graded sequence of green flashes (520 nm, light intensity graded from 10^{-4} to 10^{0}). The response to the light pulse is fast and smooth, has a sharp peak ~10 ms after the stimulus onset, settles to a low plateau, is followed by a hyperpolarization (black arrow at the bottom). (*D*) Representative receptor potential of R8H, stimulated with a graded sequence of blue flashes (440 nm, light intensity graded from 10^{-4} to 10^{0}). The response to the light pulse is larger, slower and rougher than in R1-6, starts with a peak at ~40 ms after stimulus onset, settles to a high plateau, is not followed by a hyperpolarization. (*E*) The peak-to-plateau ratio in R1-6 and R7,8. (*F*) Root mean square noise of receptor potential at half-maximal depolarization (50% V_{max}) in R1-6 and R7,8. The signal in R7,8 is noisier due to the photon shot noise, i.e. electrotonical summation of very large quantum bumps (visible at the lowest intensities in *C* and *D*). (*G*) Input resistance of R1-6 and R7,8, measured by the injection of hyperpolarizing current in discontinuous current clamp mode at 20 kHz.

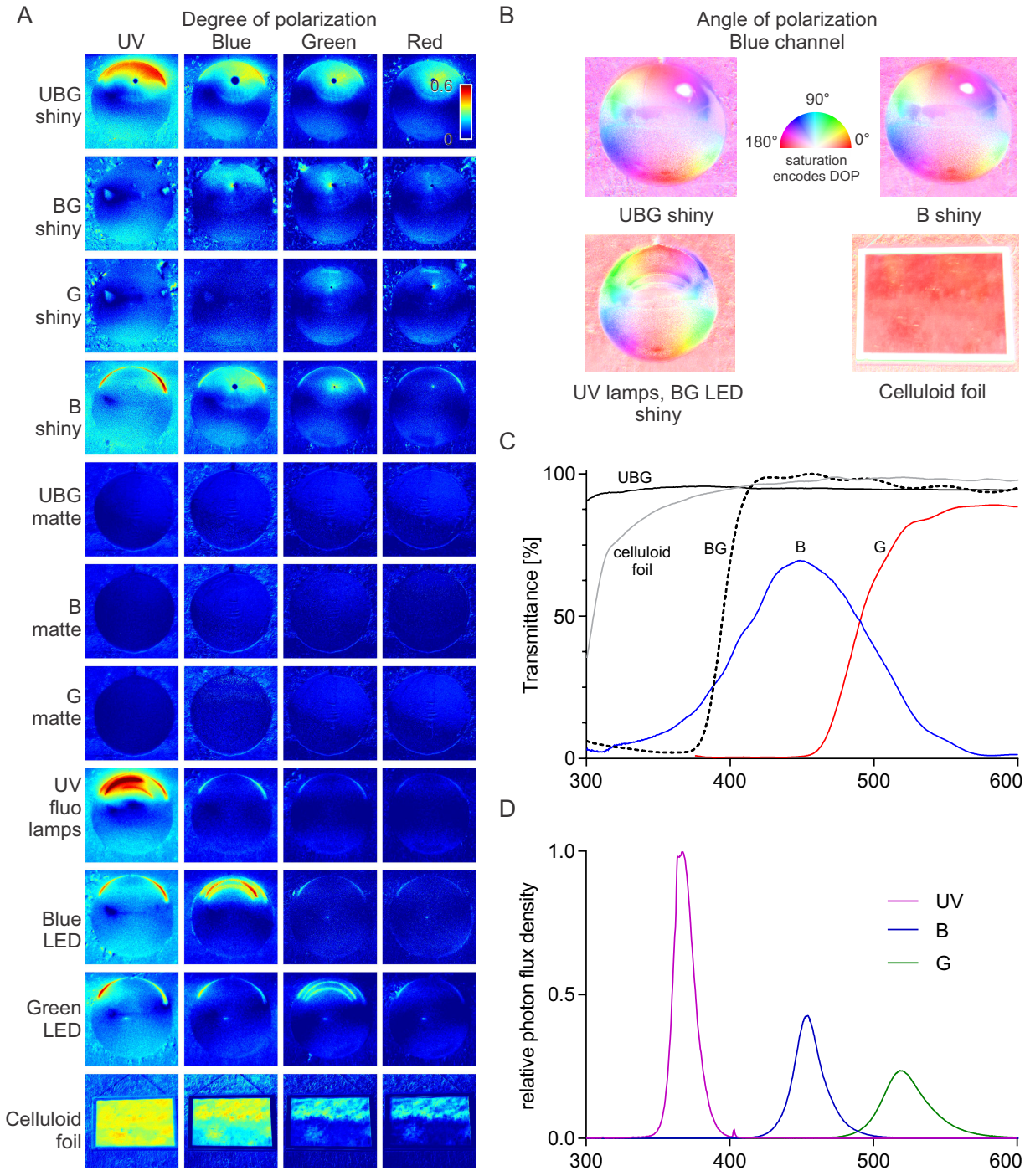

Fig. S3. Photometrical characterization of lures and filters, used in behavioral experiments.

(*A*) Degree of polarization of the combinations of shiny and matte spheres, suspended below spectral filters and electrical lamps. Images shown in UV (360±40 nm), blue (450±40 nm), green (525±40 nm) and red (600±40 nm) channel. Dark blue dots are overexposed pixels, directly reflecting the Sun. The celluloid foil at the bottom was suspended below UBG. (*B*) Angle of polarization (blue channel) of a black shiny sphere below UBG, B and LED lamps, and of the celluloid foil below UBG. (*C*) Transmittance of the spectral filters, used in (*A, B*) and of the celluloid foil. UBG, UV-transmitting plexiglass; BG, UV-blocking plexiglass; G, UV-blocking plexiglass with Lee 101 filter; B, UV-transmitting plexiglass with Lee 068 filter. (*D*) Relative irradiances of the electric lamps (UV fluorescent lamps, blue and green LED strips), used to illuminate the spheres, measured as the reflectance from a MgO standard, positioned in the location of the sphere.

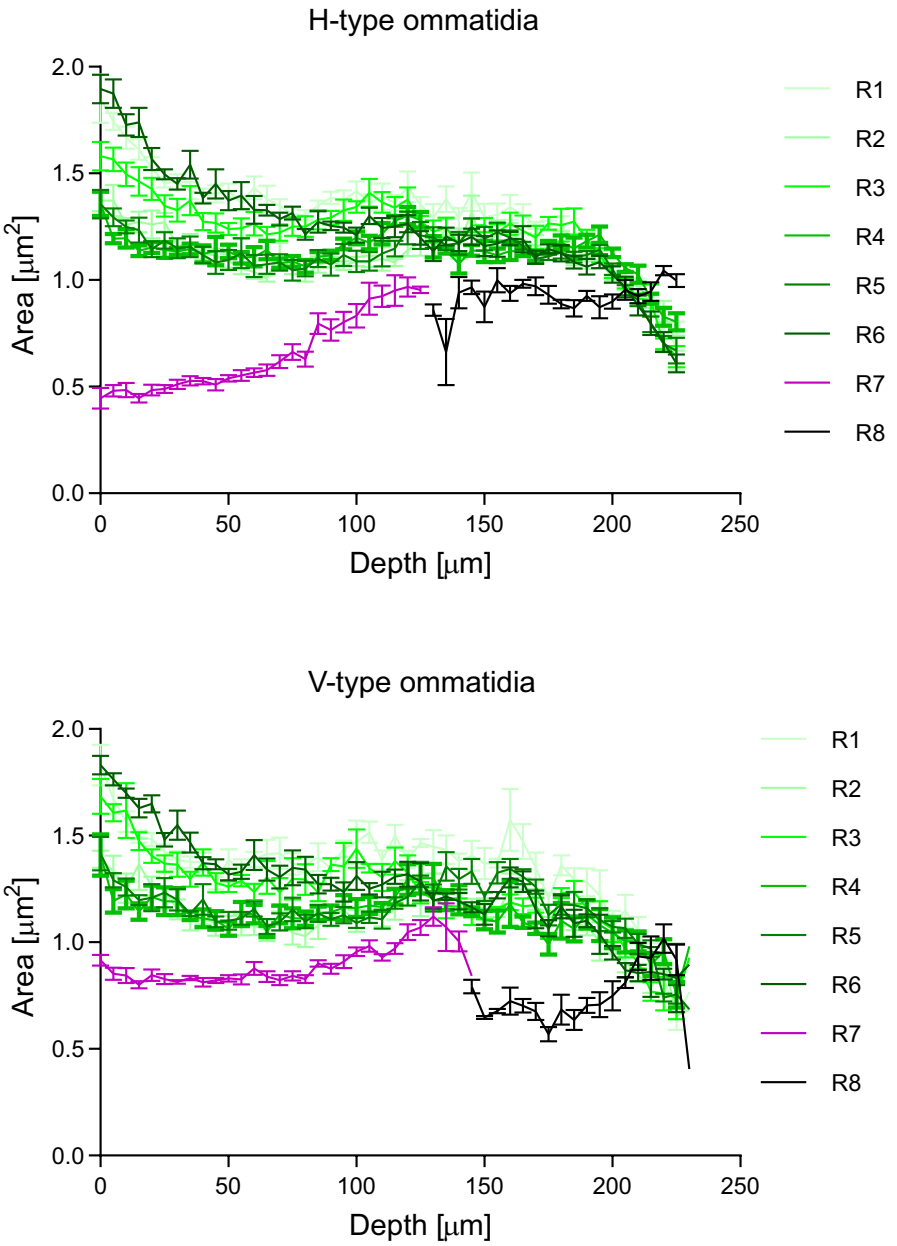

Fig. S4. Rhabdomeric cross-section area as a function of the distance from the distal tip.

Each rhabdomere of the outer photoreceptors R1-6 in both types of ommatidia is large at the distal tip (1.3-1.8 μm^2 area, corresponding to 1.28-1.51 μm diameter) and tapers proximally. Central rhabdomeres are thinner than those of R1-6. R7H rhabdomeres are distally very slender (area 0.5 μm^2, rectangular shape, width 1 μm, height 0.5 μm), but double their cross-section area proximally. H-type ommatidia, *N*=9; V-type ommatidia, *N*=6; error bars indicate SD.

Movie S1.

https://dx.doi.org/10.6084/m9.figshare.8222444

Movie S2.

https://dx.doi.org/10.6084/m9.figshare.8222444

Movie S3.

https://doi.org/10.6084/m9.figshare.9785135.v1

Dataset S1. Original serial block-face scanning electromicrographs.

https://dx.doi.org/10.6084/m9.figshare.8222444

Supplemental Materials and methods

Macrophotography (Fig. S1A)
The animal was mounted with beeswax to a micromanipulator and imaged with a USB digital microscope having a ring illuminator Dino-Lite Edge AM4515ZT (AnMo Electronics, Taiwan). A sequence of images from different focal planes was merged into a single extended depth of focus image in Adobe® Photoshop® CS5 (Adobe Systems Inc., USA).

Rhabdom fluorescence (Fig. S1E,F)
Fluorescence of rhabdomeres in an optically neutralized cornea was observed with an upright epifluorescence microscope (*Tabanus*, *Musca*: Axioskop 2, Zeiss, Germany) equipped with water immersion objectives (Zeiss Achroplan 10x0.30 and 40x0.75, Ultrafluar 40x0.60; Olympus LUMPlanFL 10x0.30, 20x0.50, 40x0.60; Lomo 30x0.90). The animals were fixed with beeswax into plastic tubes, which were then mounted either on a coverslip using putty, or centered on a two-axis goniometer arm, so that the orientation of the eye towards the objective could be adjusted. Refraction of the corneal surface was optically neutralized with water (1) so that the plane with rhabdomere tips could be focussed. We took the images using a monochrome camera (CMOS, chips IMX249 or IMX036, FLIR Imaging, Canada). We used fluorescence filter sets 01 (370/395), 09 (490/515) 15 (555/580) on the Zeiss microscope, and U-MWU (385/420), U-MWBV (440/475), U-MWIG (550/570) on the Olympus microscope; the excitation band end and the emission band start wavelengths are reported in nm. Images were processed using ImageJ software.

Polarimetric Imaging (Fig. S3A)
Polarimetric imaging was used to check the degree and angle of polarization (AOP) of horsefly lures. The images were obtained with a Phoenix 5.0 MP camera (Lucid Vision labs, Germany), based on an IMX250MZR monochrome sensor. The camera uses Sony's Polarsens technology with on-chip four different directional polarising filters (0°, 90°, 45°, and 135°) on every four pixels. The camera was fitted with a UV-transmitting objective lens FL-BC2528-VGUV (Ricoh, Japan) with a 25 mm focal length and with 4 different colour filters with 80 nm FWHM bandwidth and center wavelengths at 360 nm (with IR blocking coating; Chroma, United Kingdom), 450, 525, 600 nm (Techspec, Edmund Optics, United Kingdom). The DOP and AOP for each image were calculated using Stokes parameters, given by the camera software ArenaView (Lucid Vision labs, Germany) for each pixel quadruple. In spherical lures, AOP was continuously varied across the sphere between 0° and 180°. In the lure with celluloid foil, AOP was approximately horizontal (0°). DOP of all lures in the UV, blue and green channel is shown in Fig S3*A*; AOP, multiplied by DOP in the blue channel is shown in Fig. S3*B*.

References

1. Franceschini N (1972) Pupil and Pseudopupil in the Compound Eye of *Drosophila*. *Information Processing in the Visual Systems of Anthropods: Symposium Held at the Department of Zoology, University of Zurich, March 6–9, 1972*, ed Wehner R (Springer, Berlin, Heidelberg), pp 75-82.